Antibiotic Binding to Dizinc β-Lactamase L1 from *Stenotrophomonas maltophilia*: SCC-DFTB/CHARMM and DFT Studies†

Dingguo Xu and Hua Guo*

Department of Chemistry, University of New Mexico, Albuquerque, New Mexico 87131

Qiang Cui

Department of Chemistry and Theoretical Chemistry Institute, University of Wisconsin, Madison, Wisconsin, 53706

Received: December 19, 2006; In Final Form: January 29, 2007

A dizinc β-lactamase (L1 from *Stenotrophomonas maltophilia*) complexed with an antibiotic compound (moxalactam) has been studied using a hybrid quantum mechanical/molecular mechanical (QM/MM) approach. The QM region is described by the self-consistent charge-density functional tight binding (SCC-DFTB) model while the MM by CHARMM. The Michaelis complex, which is constructed from a recent X-ray structure of the L1 enzyme with the hydrolyzed moxalactam, is simulated by molecular dynamics. The simulation yields valuable insights into substrate-enzyme interaction, whose implications in the enzyme catalysis are discussed. Finally, the QM/MM results are compared with a high-level density functional theory study of a truncated active-site model and the agreement provides strong support for the SCC-DFTB treatment of the QM region.

I. Introduction

The primary mode of bacterial resistance to the widely used β-lactam-based antibiotics, such as penicillin, cephalosporins, and carbapenems, is based on the hydrolytic cleavage of the lactam amide (C−N) bond by bacterial β-lactamases.[1−4] The most common forms of β-lactamases (classes A, C, and D in the Ambler naming scheme)[5] employ a covalent catalysis strategy with an active-site serine residue as the nucleophile, followed by the hydrolysis of the resulting intermediate. However, class B enzymes or metallo-β-lactamases (Mβ Ls), which may be coexpressed with the serine enzymes in many bacteria, utilize directly an active-site water or hydroxide as the nucleophile. Although some β-lactamases are indigenous, the overuse and misuse of antibiotics have exerted a tremendous evolutionary pressure on bacteria to develop and strengthen their capacity for drug resistance, which poses a serious challenge to public health.[6]

To curb the increasingly menacing bacterial drug resistance, effective inhibitors of β-lactamases are highly desired. Successful compounds such as clavulanic acid are now routinely coadministered with antibiotics in clinical settings to achieve maximal antibacterial efficacy. However, these β-lactamase inhibitors are only effective for serine enzymes, and no clinically useful inhibitors of Mβ Ls have been found. This is further exacerbated by broad substrate profiles of Mβ Ls. Indeed, class B β-lactamases are known to hydrolyze almost all β-lactam based antibiotics, including the latest and most powerful addition to the arsenal, namely, carbapenems, and even some inhibitors of serine-based β-lactamases.[7] While the prevalence is still relatively low, plasmid and integron-mediated dissemination of these enzymes in opportunistic Gram-negative pathogenic microorganisms responsible for hospital-acquired infections, such as *Pseudomonas aeruginosa* and *Stenotrophomonas maltophilia*, has been observed to accelerate in recent years. The horizontal proliferation of Mβ Ls between different bacterial species could have a devastating effect for the future treatment of nosocomial infections in immuno-compromised patients.[8,9] Until now, the discovery of effective inhibitors for Mβ Ls has been greatly hampered by the lack of detailed knowledge on the mode of substrate binding as well as on their catalysis mechanisms.

SCHEME 1: Atom Definition for the L1−Moxalactam Complex and the Corresponding Binding Configuration

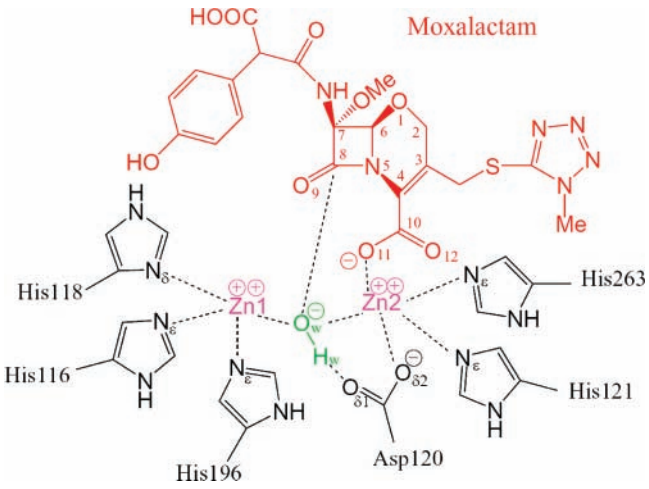

Mβ Ls are divided into three groups.[10,11] Enzymes in both B1 and B3 groups are capable of binding two zinc ions, while those in B2 are inhibited by the second zinc cofactor. They all consist of roughly 250 amino acid residues and have a similar αβ/βα fold structure, but possess diverse genetic and biochemical characteristics.[7,11] X-ray structures of enzymes in all three groups have been reported, identifying the metal-binding active sites located in the bottom of a broad crevice. Despite much

† Part of the "DFTB Special Section".

* Corresponding author. E-mail: hguo@unm.edu. Fax: 505 277 2609.

10.1021/jp068746s CCC: $37.00
Published on Web 03/03/2007

progress, there has been no report on the structure of any Michaelis complex involving an MβL and its bona fide substrate. The current experimental state of affairs has stimulated many theoretical efforts on substrate binding (see for example refs 12 and 13), but such studies have so far been found unreliable, mainly because of the difficulties in accurate description of metal−ligand interactions using force fields.[14]

The situation has greatly improved recently thanks to two important developments. First, X-ray structures of several MβLs complexed with substrate analogs have started to appear. For example, high-resolution structures of an enzyme-intermediate complex for CphA form *Aeromonas hydrophila*[15] and an enzyme−product complex for L1 from *S. maltophilia*[16] have been determined in 2005. These structures provided valuable insights into the mode of substrate binding in the active site of MβLs.

The second development is the development of hybrid QM/MM methods to investigate the substrate binding and catalysis in metallo-enzymes.[17,18] The QM/MM approach is essential because it in principle offers an reliable description of both chemical and electrostatic interactions in the active site, such as charge transfer and polarization, and is capable of handling complications, such as a change of the coordination number, during a reaction. However, such approaches are not without drawbacks. Chief among them is perhaps the steep scaling laws of the QM methods, especially for those based on first principles. The issue becomes critical for MβLs because of the necessarily large size of the QM region, which may include the metal ion(s), the protein ligands, the substrate, and the water/hydroxide nucleophile. Consequently, the QM model has to be very efficient to handle the simulations, particularly when the protein/solvent fluctuation needs be included. To this end, Merz and co-workers have developed a PM3-based QM/MM method and applied it to several metallo-enzymes.[13] The efficiency of the semiempirical PM3 method rendered it possible to simulate, for example, the binding dynamics of nitrocefin in CcrA from *Bacteroides fragilis*.[19]

In this work, we take advantage of an approximate density functional theory emerged in the past few years. The so-called self-consistent charge-density functional tight binding (SCC-DFTB) model[20] is not only reasonably accurate, but also quite efficient, with a speed comparable to other semiempirical methods such as AM1 and PM3. The SCC-DFTB model has been extensively tested[21−24] and applied successfully to several important enzymatic systems,[25−28] including β-lactamases.[29−31]

We focus here on the L1 enzyme from *S. maltophilia*, a representative member of the B3 group. This enzyme is an important source of drug resistance and has a very broad substrate profile, hydrolyzing nearly all β-lactam compounds.[32] The L1 enzyme is unique among the MβLs in that it is a tetramer and has a substantially longer peptide chain. Like its B1 and other B3 counterparts, the active site features two binding sites for zinc cofactors. The X-ray structure of the apo enzyme[33] shows that the first metal cofactor (Zn1) is coordinated by three histidine ligands (His116, His118 and His196), while the second (Zn2) by Asp120, His121, and His263, and an "apical" water. In addition, the two metal ions are bridged by an oxygen moiety that is widely believed to be a hydroxide ion and the nucleophile in the hydrolysis reaction.[33]

Our work reported here was motivated by a recent crystal structure of L1 complexed with the hydrolysis product of moxalactam by Spencer et al.,[16] which provided some important clues on the mode of substrate binding. We describe here a manual procedure to reconstruct unambiguously the Michaelis complex based on the X-ray structure and a QM/MM simulation of the active site dynamics based on a SCC-DFTB/CHARMM protocol. Such a study is important for understanding the mode of substrate binding of MβLs in general and for gaining insight into the factors that influence the catalysis of dizinc MβLs. This publication is organized as follows. Section II describes the theoretical methods used in our simulations and the procedure for reconstructing the Michaelis complex. Section III presents the simulation results with a comparison with known experimental facts and a discussion on the implications in enzyme catalysis. The final section (Section IV) concludes.

II. Theory

A. SCC-DFTB-Based QM/MM. The hybrid quantum mechanical and molecular mechanical (QM/MM) approach has become the method of choice in studying macromolecular systems such as enzymes.[34−40] The basic idea is to separate the system to two parts: treating a small reactive region with accurate quantum mechanics while approximating the surrounding with a classical force field. This is necessary because the bond breaking and bond forming processes cannot be easily modeled by a force field, while a full quantum treatment of the enzymatic system and solvent is formidable. As discussed earlier, the QM/MM approach is particularly relevant for metallo-enzymes because of the difficulties associated with the force-field description of the metal−ligand bonds.[14]

Ideally, the QM part of the calculation should be treated with ab initio methods such as Hartree−Fock or density functional theory (DFT). However, the numerical costs of an ab initio QM/MM approach restrict its application to systems involving a small QM region.[39] In our case, the QM region has 125 atoms, including the two zinc ions, the putative hydroxide nucleophile bridging the two metal ions, the side chains of the six protein ligands (His116, His118, His196, Asp120, His121, and His263), and the entire substrate. The large number of electrons in our system thus precludes an ab initio approach.

In this work, we took advantage of the recent developed SCC-DFTB method to provide a highly efficient and reasonably accurate description of the QM region. Because the SCC-DFTB approach has been extensively described in the literature,[20] only a brief review is given here. Essentially, SCC-DFTB is an approximate density functional theory, which approximates the total energy with a second-order expansion in terms of the charge density variation with respect to a reference density. It represents an improvement of the original DFTB method because of a self-consistent procedure which iteratively relaxes the atomic Mulliken charges. The total energy of the system in SCC-DFTB is given by

$$E^{\mathrm{SCC-DFTB}} = \sum_{i}^{\mathrm{occ}} \langle \phi_i | \hat{H}_0 | \phi_i \rangle + \frac{1}{2} \sum_{\mathrm{A,B}} \gamma_{\mathrm{AB}} \Delta q_{\mathrm{A}} \Delta q_{\mathrm{B}} + E_{\mathrm{rep}} \tag{1}$$

where $\hat{H}_0$ is the effective Kohn−Sham Hamiltonian and ϕ_i are the Kohn−Sham orbitals. Δq_{A} (Δq_{B}) is the Mulliken charge fluctuation of atom A (B) relative to the number of valence electrons in its neutral state, and γ_{AB} is a function that approximates the second derivative with respect to the charge fluctuation. The energy expression in eq 1 has an important semiempirical component, namely, the pairwise repulsive potential (E_{rep}), which is fitted to high level DFT results of reference systems. The SCC-DFTB approach is very efficient, with a speed comparable to other semiempirical methods such as AM1 and PM3. The efficiency of the SCC-DFTB method

partially derives from this pairwise term, but also from the fact that the elements of the Hamiltonian and overlap matrices are approximated by two-center integrals, which are interpolated from precalculated points.

Extensive tests have validated the viability of the SCC-DFTB method in describing molecular geometry,[21,23] vibrational frequencies,[24] and reaction energies[21−23] of many molecular systems. Extensive comparisons of molecular geometries have shown that the SCC-DFTB method typically reproduces B3LYP/6-31G(d,p) bond lengths and bond angles within a few hundredths of Å and a few degrees, respectively.[21,23] The average error in the reaction energy is on the order of only a few kcal/mol.[21,23] In addition, recent work has shown that the vibrational frequencies for a set of 66 molecules calculated by the SCC-DFTB method have an average deviation of 57 cm^{-1} from experimental values,[24] similar to those obtained from the B3LYP/cc-pVDZ level of theory and significantly better than the AM1 and PM3 models.

As a result, the SCC-DFTB method has been applied to many biological systems with impressive results.[21,22,25−27,41−46] A particularly important recent advance related to this work is the parametrization of the zinc ion in biological systems, which yielded results such as geometries and ligand binding energies that are in much better agreement with the B3LYP/6-311+G** results than other semiempirical methods.[45]

The SCC-DFTB method has been implemented by one of the authors[21] in the CHARMM suite of simulation codes.[47] In this implementation, the MM portion of the system is described by the CHARMM all atom force field[48] and the QM-MM interface was approximated by link atoms,[34,35] which interact with all MM atoms except the link hosts. In this work, we have six link atoms connected with the C_β atoms of the corresponding protein ligands with the C_α atoms as the link hosts. The CHARMM van der Waals parameters were used for all QM atoms.

B. Simulation Protocol. The starting structure used in our simulations was based on the recently reported X-ray structure of L1 complexed with a hydrolysis product of moxalactam (PDB code 2AIO).[16] In this X-ray structure, a bridging oxygen atom exists between the two zinc cofactors. This moiety was modeled as the OH^- anion which serves as the putative nucleophile. In addition, the two zinc ions are coordinated by His116, His118, His196 in the Zn1 site and His121, His263, and Asp120 in the Zn2 site. In our simulation, the Asp120 side chain is in the ionized form, based on previous theoretical work.[29,49,50] The total charge of the QM region is thus zero.

The Michaelis complex was constructed from the 2AIO structure. To this end, we modified the X-ray structure following a similar approach detailed in our earlier work.[30] The anchoring point of our docking model is the carboxylate group in the C_4 position of the substrate, which has been shown in the X-ray structure to be one of metal ligands in the Zn2 site.[16] Since this carboxylate is conserved in all β-lactam antibiotics, its importance in substrate binding is self-evident. As a result, its direct metal coordination is preserved in our model.

Our procedure consists of three steps. First, all crystal water molecules in the X-ray structure were removed from the enzyme active site. The moxalactam substrate was then recovered from the hydrolysis product by replacing the C_8 carboxylate group by carbonyl and by reconnecting the amide C−N bond in the lactam ring. In addition, the 1-methyltetrazolyl-5-thiolate group missing in the X-ray structure was reattached. Finally, a very short steepest decent minimization of the QM region was performed to relax the system. By doing so, the C_4−carboxylate coordination to Zn2 is preserved with minimal structural disturbance. This procedure was found to be quite robust in generating the initial structure for MD simulations.

Once the model enzyme−substrate complex was constructed, it was solvated by a pre-equilibrated sphere of TIP3P waters[51] with a 25 Å radius centered at the zinc bridging hydroxide. Any water molecule found within a 2.8 Å radius of a heavy protein/substrate atom was deleted. Subsequently, the solvent was relaxed with a 30 ps molecular dynamics (MD) run with all protein and substrate atoms fixed in their original positions. This process was repeated several times with randomly rotated water spheres to ensure even solvation.

To reduce the computational cost, stochastic boundary conditions[52] were applied to the enzyme−substrate complex. Atoms in the reaction zone, defined by a radius of 22 Å, were subjected to Newtonian dynamics on the combined QM/MM potential, while atoms that are more than 25 Å away from the zinc bridging hydroxide were removed. In between, atoms in the buffer zone were subjected to Langevin dynamics with frictions and random forces to simulate the influence of the bulk that was not included in the simulation. The total number of atoms in our system is 7195, in which there are 1253 water molecules.

The energy of the system was first minimized using the steepest decent method to remove bad contacts, and further by the adapted basis Newton−Raphson method. The optimized structure was taken to be the initial conditions for MD. During the MD simulation, the temperature was slowly increased to room temperature (300 K) and the system was allowed to equilibrate for 100 ps. The total length of the MD trajectory was 350 ps. The MD simulation employed an integration step of 1.0 fs with the SHAKE algorithm[53] for covalent bonds connected to a hydrogen atom. Throughout the simulation, the group based switching approach[54] was applied to treat the nonbonded interactions. All QM/MM simulations were performed with the CHARMM suite of molecular simulation codes.[47]

C. DFT with Truncated Active Site Models. To verify the SCC-DFTB/CHARMM approach outlined above, we have also performed a high-level DFT study of a truncated active-site model. In such a model, the His and Asp residues were approximated by methyl imidazole and acetate, respectively. The substrate was mimicked by a moxalactam analog, which replaces the 7b-[(4-hydroxyphenyl)malonyl]-amino group with a hydrogen atom and the 1-methyl-5-thiotetrazole by methyl group. The calculation employed the Becke3−Lee−Yang−Parr (B3LYP) exchange-correlation functional[55,56] with a standard basis set (6-31G(d)), as implemented in Gaussian 03.[57] Geometry optimization was carried out with the initial configuration generated by the minimal energy structure in the QM/MM simulation.

III. Results

An important issue in the simulations is concerned with the treatment of electrostatic interactions. A common QM/MM protocol calls for untruncated QM-MM electrostatic interactions, but such interactions between MM atoms are typically truncated at a pre-specified distance, say 12 Å. Such an imbalance could result in unnecessarily large interactions between atoms in the QM and MM regions. Indeed, we have found that the binding between the substrate and the enzyme was unstable when the electrostatic interactions among MM atoms were truncated. Water molecules, which were treated in our simulations as classical particles (TIP3P), eventually came between the sub-

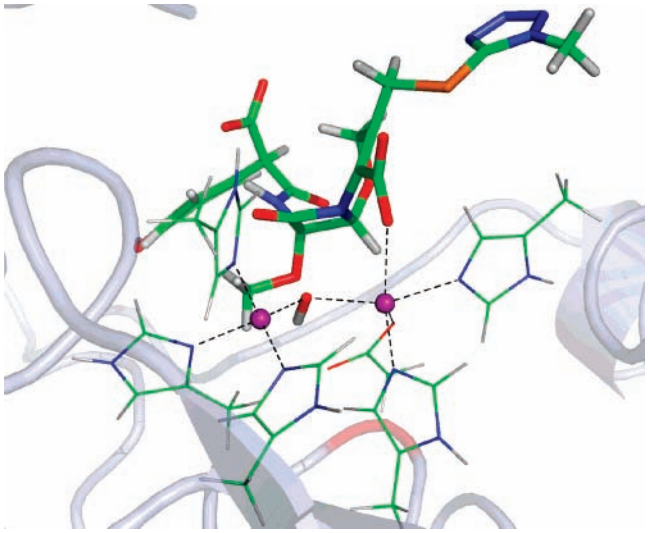

Figure 1. Snapshot of the active site obtained from the QM/MM simulation of the L1-moxalactam complex. The substrate is depicted by heavy tubes while the protein ligands by thin ones. The ligand−metal bonds are indicated by dash lines.

strate and metal ions. This artifact was corrected when the long-range interactions in the MM region were included in the group based approach. The importance of long-range electrostatic interactions found in this study is consistent with our earlier observations in carbonic anhydrase.[40,58]

Overall, the L1−moxalactam complex was found to be quite stable during the 250 ps MD simulation, as evidenced by the small (0.76 ± 0.05 Å) root-mean-square deviation (rmsd) of the protein backbone atoms. A snapshot of the active site of enzyme−substrate complex is given in Figure 1. The corresponding averaged internuclear distances and bond angles are listed in Table 1, with comparison with available experimental data and the DFT results.

In agreement with the X-ray structure, the metal ion in the Zn1 position is tetra-coordinated, while that in the Zn2 site is penta-coordinated. The four Zn1 ligands consist of the three histidine residues (His116, His118, and His196) and the bridging hydroxide. On the other hand, the five ligands of Zn2 include the bridging hydroxide, His121, His263, Asp120, and the C_4−carboxylate group from the substrate moxalactam. The experimental distances between the protein ligands and the metal ions are mostly reproduced well by the simulation, as shown in Table 1. The only exception is His116, whose N_ϵ−Zn1 distance was found in the simulation to be 2.04 ± 0.06 Å, comparable to N−Zn distances for other His ligands. However, this distance is much smaller than the experimental value of 2.20 Å.[16] The origin of the discrepancy is not clear. Similarly, the experimental angles in the metal centers were found to fluctuate around values that are very close to experimental data, as shown in Table 1.

The position and orientation of the hydroxide nucleophile are important factors in the preorganization of the near-attack configuration in the Michaelis complex. The distance between the two zinc ions was found to be 3.63 ± 0.11 Å, which compares well with the experimental distance of 3.68 Å.[16] The experimentally observed Zn1−O_w−Zn2 angle of 125.1° (ref 16) is also well reproduced by the simulation (126.0 ± 6.6°). In addition, the hydroxide was found to be slightly closer to Zn1 (1.97 ± 0.05 Å) than to Zn2 (2.11 ± 0.08 Å), in excellent agreement with the experimental values of 1.98 Å and 2.15 Å.[16] This asymmetry is presumably due to the penta-coordination of the Zn2 ion. As suggested by the X-ray structures,[16,33] the hydroxide was found to form a hydrogen bond with Asp120,

TABLE 1: Comparison of Theoretical and Experimental Geometrical Parameters for L1−Moxalactam Complex

distance (Å)/angle (deg)	DFT	QM/MM MD	exp.[16]
O_w···C_8	5.70	2.87 ± 0.24	−
N_5···Zn2	4.84	3.10 ± 0.19	2.38
O_{11}···Zn2	2.20	2.34 ± 0.19	2.30
O_w···Zn1	1.90	1.97 ± 0.05	1.98
O_w···Zn2	1.96	2.11 ± 0.08	2.15
O_9-Zn1	5.00	3.54 ± 0.31	−
O_{11}···H_γ(Ser221)	−	1.75 ± 0.12	2.69[a]
O_{12}···H_γ(Ser223)	−	1.72 ± 0.12	2.66[a]
H_w···$O_{\delta1}$(Asp120)	1.67	1.89 ± 0.13	−
Zn1-Zn2	3.73	3.63 ± 0.11	3.68
Zn1···N_δ(His118)	2.03	2.05 ± 0.06	2.08
Zn1···N_ϵ(His116)	2.02	2.04 ± 0.06	2.20
Zn1···N_ϵ(His196)	2.03	2.02 ± 0.06	2.07
Zn2···$O_{\delta2}$(Asp120)	2.18	2.17 ± 0.08	2.19
Zn2···N_ϵ(His121)	2.05	2.05 ± 0.05	2.08
Zn2···N_ϵ(His263)	2.07	2.11 ± 0.09	2.10
Zn1···O_w···Zn2	150.3	126.0 ± 6.6	125.1
O_w···Zn1···$N_{\epsilon2}$(His116)	110.5	114.7 ± 6.5	97.2
O_w···Zn1···$N_{\delta1}$(His118)	107.2	116.5 ± 5.5	111.6
O_w···Zn1···$N_{\epsilon2}$(His196)	108.5	116.9 ± 6.0	135.9
O_w···Zn2···O_{11}	94.1	86.4 ± 6.5	91.3
O_w···Zn2···$N_{\epsilon2}$(His263)	129.0	154.7 ± 8.4	166.4
O_w···Zn2···$N_{\epsilon2}$(His121)	116.2	97.3 ± 5.5	97.2
O_w···Zn2···$O_{\delta2}$(Asp120)	90.3	91.4 ± 5.6	84.5
O_w···H_w···$O_{\delta1}$(Asp120)	171.5	137.0 ± 11.0	−
N_ϵ(His263) ···Zn2···N_e(His121)	114.6	106.7 ± 6.9	96.3
N_ϵ(His263) ···Zn2··$O_{\delta2}$(Asp120)	85.8	84.6 ± 4.5	93.2
N_ϵ(His121) ···Zn2····$O_{\delta2}$(Asp120)	90.4	103.0 ± 5.5	92.7
$N_{\delta1}$(His118) ···Zn1···N_{e2}(His116)	113.2	98.0 ± 4.6	99.4
$N_{\delta1}$(His118) ···Zn1···N_{e2}(His196)	106.2	110.4 ± 5.1	107.9

[a] The distances from O_{11}/O_{12} to the O_γ atoms of Ser221/223.

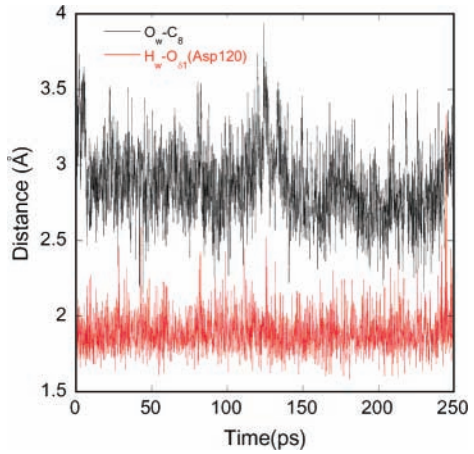

Figure 2. The distance between the hydroxide hydrogen (H_w) and the nonmetal-bound oxygen ($O_{\delta1}$) of Asp120 in the enzyme−substrate complex and the distance between the nucleophilic oxygen (O_w) and the lactam carbonyl carbon (C_8).

as evidenced by the H_w-$O_{\delta1}$ distance of 1.89 ± 0.13 Å. The fluctuation of this key hydrogen bond distance is given in Figure 2.

According our docking model based on the X-ray structure, the substrate binds to the enzyme through two important anchoring points. One is the direct ligation of Zn2 by the substrate C_4−carboxylate group. Such a direct substrate-metal interaction has been seen in the X-ray structure,[16] and supported by spectroscopic[59−61] and binding studies.[62] The O_{11}-Zn2 distance obtained from our simulation is 2.34 ± 0.19 Å, which is very close to the experimental value of 2.30 Å.[16] The other primary binding determinant is the hydrogen bonds of both C_4−carboxylate group oxygen atoms with the side chains of Ser223 and Ser221, respectively. The corresponding O−H distances

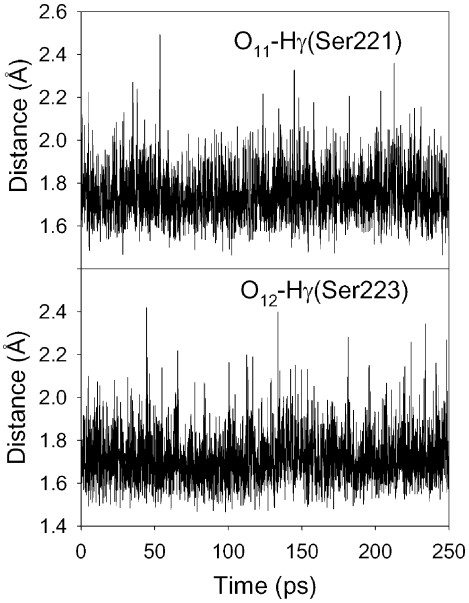

Figure 3. The hydrogen bond distances between the C_4−carboxylate oxygen atoms and the hydrogen atoms of Ser221 and Ser223.

are shown in Figure 3, and their averages of 1.72 ± 0.12 and 1.75 ± 0.12 Å indicate strong hydrogen bonds. The serine residues are unique for L1, but they can be considered as analogs of a mostly conserved lysine residue (Lys224) in many other MβLs, such as CcrA[63,64] and CphA.[15] The role of this lysine residue in substrate binding is well established, and has recently been exploited in designing a new antibiotic strategy.[65] In L1, kinetic data indicated that mutations of the serine residues typically increase K_M and decreases k_{cat}, but the exact amount depends on the substrate.[66]

Another hydrogen bond exists between the phenyl hydrogen of Tyr32 and the carbonyl carbon of the 7β-[(4-hydroxyphenyl)-malonyl]-amino group of the substrate, as evidenced by the hydrogen bond distance of 1.77 ± 0.16 Å. This is consistent with the observed O−O distance of 2.83 Å in the X-ray structure.[16]

In addition to the two strong anchoring points mentioned above, the substrate might be further stabilized by the flexible loop made up of residues 156−162.[33] In particular, the X-ray structure of Spencer et al.[16] has shown that the 7β-[(4-hydroxyphenyl)malonyl]-amino group of the substrate interacts with the side chains of Phe156, Ile162, and Tyr32. These hydrophobic interactions are maintained in our simulation. Fluorescence measurements of L1 confirms the involvement of the flexible loop,[67] but its effects on the catalysis was found to be relatively small.[66,68] Interestingly, the position of this loop changes little before and after substrate binding, as clearly seen in Figure 4, where the backbone of the apo enzyme (1SML)[33] is compared with that of L1 complexed with the product of moxalactam hydrolysis (2AIO).[16] Unfortunately, the time scale of our MD simulation is too short to capture possible conformational changes in the substrate binding process. In contrast to the hydrophobic interactions surrounding the 7β-[(4-hydroxyphenyl)malonyl]-amino group, the 1-methyl-5-thiotetrazole group at the C_3 position is completely solvated by the water solvent.

The mode of substrate binding based on the direct interaction between C_4−carboxylate and the Zn/Ser (or Zn/Lys) moieties is believed to be quite common for all MβLs, as suggested by recent X-ray structures[15,16] and confirmed by several theoretical simulations.[19,30,69,70] The direct carboxylate-metal binding has

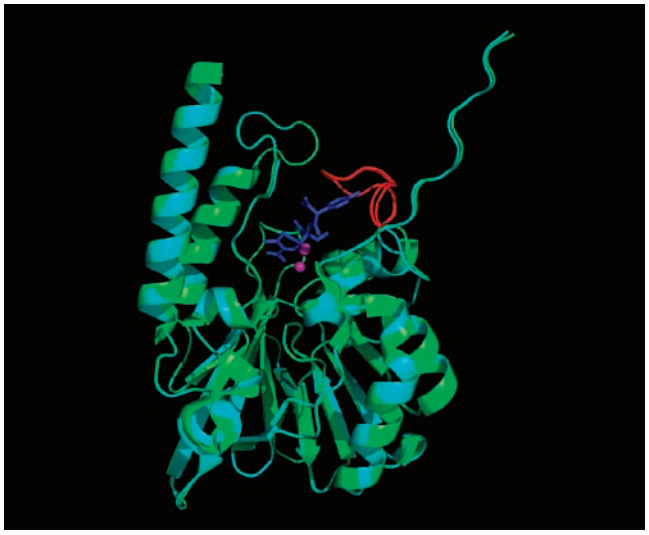

Figure 4. Overlay of the structures of the apo L1 enzyme (green) and the enzyme-intermediate complex (light blue). Metal ions and the intermediate molecule are colored in purple and dark blue, respectively. The flexible loop consisting of the 156−162 residues is colored red.

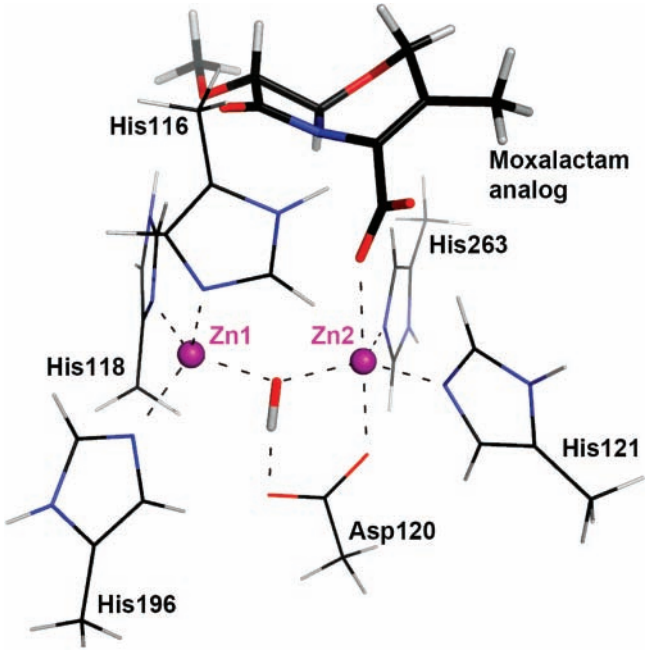

Figure 5. Geometry of the truncated active-site model obtained at the B3LYP/6-31G(d) level of theory. The carbon, nitrogen, oxygen, zinc, and hydrogen atoms are colored as black, blue, red, purple, and gray, respectively. The ligand−metal and hydrogen bonds are indicated by dash lines.

also been seen in MβLs complexed with substrate analogs.[71,72] Since the C_4−carboxylate moiety is functionally conserved in all β-lactam antibiotics, the binding pattern is consistent with the observed broad substrate profile of MβLs.[7] Among the two, the metal binding is probably the dominant one because site-directed mutations of Ser223 in L1 was found to impact substrate binding only marginally.[66]

The bridging hydroxide is well positioned for its nucleophilic attack of the carbonyl carbon (C_8) in the substrate lactam ring. Indeed, the O_w−C_8 distance was found to be 2.87 ± 0.24 Å in our simulation, as shown in Figure 2. The orientation of the OH^- nucleophile is largely maintained by its hydrogen bond with the metal-bound Asp120, whose distance is also shown in the same figure. The metal binding Asp120 is known to play a crucial role in both substrate binding and catalysis of L1.[73]

According to the commonly accepted mechanism,[2,4] the hydrolysis reaction is initiated by the nucleophilic attack of the lactam carbonyl carbon by the hydroxide nucleophile. This might be assisted by the polarization of the carbonyl oxygen (O_9) by Zn1, as the O_9-Zn1 distance is only 3.54 ± 0.31 Å in the Michaelis complex and expected to decrease as the nucleophile approaches its target. In other words, Zn1 might serve as an oxyanion hole to stabilize the negative charge buildup at the carbonyl oxygen atom (O_9). The nucleophilic attack would result in the cleavage of the lactam ring and the production of a negatively charged nitrogen, which is believed to be stabilized by the metal ion in the Zn2 position. Our simulation supports the viability of this scenario because the lactam nitrogen (N_5) is not far from Zn2, with a distance of 3.10 ± 0.19 Å. In addition, the carboxylate group resulted from the nucleophilic addition of the hydroxide can easily be stabilized by the metal ion in the Zn1 position. In the final step of the proposed mechanism, the anionic nitrogen needs to be protonated, probably by Asp120, to yield the product. Overall, the active-site geometry of our model Michaelis complex provides strong support to the proposed mechanism.

The active-site geometry of the Michaelis complex revealed by the QM/MM simulation was confirmed by our truncated active-site model at the B3LYP/6-31G(d) level of theory. The optimized structure of the truncated model is shown in Figure 3, and the geometric parameters are compared with the QM/MM and experimental data in Table 1. Although differences do exist, the overall agreement between the two theoretical models is quite satisfactory. For instance, both models predict the tetrahedral coordination at the Zn1 site, and the pentacoordination at the Zn2 site. The Zn−Zn distance in the truncated model is slightly larger (3.73 Å) than that in the QM/MM simulation (3.63 ± 0.11 Å), which can presumably be attributed to the lack of the enzyme environment in the former case. In both models, the O−Zn distances reproduce experimental data quite well. In addition, the DFT result confirms the hydrogen bond between the nucleophilic hydroxide with the Asp120, and the corresponding $H_w-O_{\delta 1}$ distance (1.85 Å) is almost identical to the QM/MM value (1.89 ± 0.13 Å). The distance between the nucleophilic oxygen (O_w) and its target (C_8) in the truncated active-site model is larger than that from QM/MM simulation, but this is not unreasonable because neither solvent and the remaining part of the protein was included in the DFT calculation. The overall agreement provided important supporting evidence for the validity of the SCC-DFTB description of the active site in the QM/MM simulation.

IV. Conclusion

In this work, we have investigated the active-site dynamics of a metallo-β-lactamase (L1) complexed with a β-lactam antibiotic molecule (moxalactam) using a recently developed QM/MM approach. In particular, we have used the SCC-DFTB method to describe the metal cofactors and its protein ligands, the putative nucleophile, and the entire substrate. The number of QM atoms in the dizinc L1 is significantly larger than that in our earlier work on monozinc CphA.[30,31] The structural and dynamical information extracted from a 350 ps MD simulation shows an excellent agreement with both experimental data and high level DFT results based on a truncated active-site model. The results presented here provide further support for the reliability of the SCC-DFTB approach for molecular structural characterization, particularly for enzymatic systems with zinc cofactors.

The current model for the Michaelis complex of the L1 enzyme from *S. maltophilia* is much less ambiguous than many previous models because it is based on a recent X-ray structure that identified several important binding determinants for β-lactam antibiotics. In particular, the substrate binds directly with a zinc ion in the Zn2 position with its C_4-carboxylate, an observation that supports the direct involvement of the metal cofactor in substrate binding. The same C_4-carboxylate moiety was also found to form strong hydrogen bonds with Ser221 and Ser223, which might further stabilize the substrate in the active site. The prominent role played by C_4-carboxylate in binding is consistent with the facts that this moiety is functionally conserved in all β-lactam antibiotics and that all B1 and B3 MβLs have broad substrate profiles.

The QM/MM MD simulation revealed a well organized active site, featuring two zinc ions bridged by a hydroxide ion. This putative nucleophile is not only reasonably close to its target, namely the carbonyl carbon in the substrate lactam ring, but also oriented by a hydrogen bond to Asp120 for an optimal approach. The geometry of the substrate in the Michaelis complex supports the proposed catalytic mechanism. For instance, the lactam nitrogen, which is proposed to be stabilized by a metal ion in a reaction intermediate, is located sufficiently close for such an interaction. The study reported in this work set the stage for future investigations of the reaction mechanism.

Acknowledgment. This work was supported by National Institutes of Health (R03AI068672) and National Science Foundation (MCB-0313743). QC acknowledges National Science Foundation (MCB-0314327). Some of the calculations were carried out at the National Centers for Supercomputing Applications (NCSA).

References and Notes

(1) Knowles, J. R. *Acc. Chem. Res.* **1985**, *18*, 97.
(2) Wang, Z.; Fast, W.; Valentine, A. M.; Benkovic, S. J. *Curr. Opin. Chem. Biol.* **1999**, *3*, 614.
(3) Fisher, J. F.; Meroueh, S. O.; Mobashery, S. *Chem. Rev.* **2005**, *105*, 395.
(4) Crowder, M. W.; Spencer, J.; Vila, A. J. *Acc. Chem. Res.* **2006**, *45*, 13650.
(5) Ambler, R. P. *Philos. Trans. R. Soc. London* **1980**, *B289*, 321.
(6) Neu, H. C. *Science* **1992**, *257*, 1064.
(7) Bush, K. *Clin. Infect. Dis.* **1998**, *27*, S48.
(8) Payne, D. J. *J. Med. Microbiol.* **1993**, *39*, 93.
(9) Walsh, T. R.; Toleman, M. A.; Poirel, L.; Nordmann, P. *Clin. Micobiol. Rev.* **2005**, *18*, 306.
(10) Bush, K.; Jacoby, G. A.; Medeiros, A. A. *Antimicrob. Agents. Chemother.* **1995**, *39*, 1211.
(11) Galleni, M.; Lamotte-Brasseur, J.; Rossolini, G. M.; Spencer, J.; Dideberg, O.; Frere, J.-M. *Antimicrob. Agents Chemother.* **2001**, *45*, 660.
(12) Olsen, L.; Antony, J.; Hemmingsen, L.; Mikkelsen, K. V. *J. Phys. Chem.* **2002**, *A106*, 1046.
(13) Estiu, G.; Suarez, D.; Merz, K. M., Jr. *J. Comput. Chem.* **2006**, *27*, 1240.
(14) Park, H.; Merz, K. M., Jr. *J. Med. Chem.* **2005**, *48*, 1630.
(15) Garau, G.; Bebrone, C.; Anne, C.; Galleni, M.; Frere, J.-M.; Dideberg, O. *J. Mol. Biol.* **2005**, *345*, 785.
(16) Spencer, J.; Read, J.; Sessions, R. B.; Howell, S.; Blackburn, G. M.; Gamblin, S. J. *J. Am. Chem. Soc.* **2005**, *127*, 14439.
(17) Peters, M. B.; Raha, K.; Merz, K. M., Jr. *Curr. Opin. Drug Disc. Dev.* **2006**, *9*, 370.
(18) Cavalli, A.; Carloni, P.; Recanatini, M. *Chem. Rev.* **2006**, *106*, 3497.
(19) Park, H.; Brothers, E. N.; Merz, K. M., Jr. *J. Am. Chem. Soc.* **2005**, *127*, 4232.
(20) Elstner, M.; Porezag, D.; Jungnickel, G.; Elsner, J.; Haugk, M.; Frauenheim, T.; Suhai, S.; Seigert, G. *Phys. Rev.* **1998**, *B58*, 7260.
(21) Cui, Q.; Elstner, M.; Kaxiras, E.; Frauenheim, T.; Karplus, M. *J. Phys. Chem. B* **2001**, *105*, 569.
(22) Elstner, M.; Hobza, P.; Frauenheim, T.; Suhai, S. *J. Chem. Phys.* **2001**, *114*, 5149.
(23) Pu, J.; Gao, J.; Truhlar, D. G. *J. Phys. Chem.* **2004**, *A108*, 5454.
(24) Witek, H. A.; Morokuma, K. *J. Comput. Chem.* **2004**, *25*, 1858.
(25) Cui, Q.; Elstner, M.; Karplus, M. *J. Phys. Chem. B* **2002**, *106*, 2721.

(26) Elstner, M.; Jalkanen, K. J.; Knapp-Mohammady, M.; Frauenheim, T.; Suhai, S. *Chem. Phys.* **2001**, *263*, 203.
(27) Zhang, X.; Harrison, D. H.; Cui, Q. *J. Am. Chem. Soc.* **2002**, *124*, 14871.
(28) Guo, H.; Rao, N.; Xu, Q.; Guo, H. *J. Am. Chem. Soc.* **2005**, *127*, 3191.
(29) Gu, W.; Zhu, J.; Liu, H. *J. Theo. Comp. Chem.* **2002**, *1*, 62.
(30) Xu, D.; Zhou, Y.; Xie, D.; Guo, H. *J. Med. Chem.* **2005**, *48*, 6679.
(31) Xu, D.; Xie, D.; Guo, H. *J. Biol. Chem.* **2006**, *281*, 8740.
(32) Crowder, M. W.; Walsh, T. R.; Banovic, L.; Pettit, M.; Spencer, J. *Antimicrob. Agents Chemother.* **1998**, *42*, 921.
(33) Ullah, J. H.; Walsh, T. R.; Taylor, I. A.; Emery, D. C.; Verma, C. S.; Gamblin, S. J.; Spencer, J. *J. Mol. Biol.* **1998**, *284*, 125.
(34) Warshel, A.; Levitt, M. *J. Mol. Biol.* **1976**, *103*, 227.
(35) Field, M. J.; Bash, P. A.; Karplus, M. *J. Comput. Chem.* **1990**, *11*, 700.
(36) Gao, J. *Acc. Chem. Res.* **1996**, *29*, 298.
(37) Monard, G.; Merz, K. M., Jr. *Acc. Chem. Res.* **1999**, *32*, 904.
(38) Warshel, A. *Annu. Rev. Biophys. Biomol. Struct.* **2003**, *32*, 425.
(39) Friesner, R. A.; Guallar, V. *Annu. Rev. Phys. Chem.* **2005**, *56*, 389.
(40) Riccardi, D.; Schaefer, P.; Yang, Y.; Yu, H.; Ghosh, N.; Prat-Resina, X.; Konig, P.; Li, G.; Xu, D.; Guo, H.; Elstener, M.; Cui, Q. *J. Phys. Chem. B* **2006**, *110*, 6458.
(41) Elstner, M.; Jalkanen, K. J.; Knapp-Mohammady, M.; Frauenheim, T.; Suhai, S. *Chem. Phys.* **2000**, *256*, 15.
(42) Elstner, M.; Frauenheim, T.; Kaxiras, E.; Seifert, G.; Suhai, S. *Phys. Status Solidi* **2000**, *B217*, 357.
(43) Guo, H.; Cui, Q.; Lipscomb, W. N.; Karplus, M. *Proc. Natl. Acad. Sci. U.S.A.* **2001**, *98*, 9032.
(44) Li, G.; Cui, Q. *J. Am. Chem. Soc.* **2003**, *125*, 15028.
(45) Elstner, M.; Cui, Q.; Munih, P.; Kaxiras, E.; Frauenheim, T.; Karplus, M. *J. Comput. Chem.* **2003**, *24*, 565.
(46) Riccardi, D.; Schaefer, P.; Cui, Q. *J. Phys. Chem. B* **2005**, *109*, 17719.
(47) Brooks, B. R.; Bruccoleri, R. E.; Olafson, B. D.; States, D. J.; Swaminathan, S.; Karplus, M. *J. Comput. Chem.* **1983**, *4*, 187.
(48) MacKerell, A. D., .Jr.; Bashford, D.; Bellott, M.; Dunbrack, R. L., Jr.; Evanseck, J. D.; Field, M. J.; Fischer, S.; Gao, J.; Guo, H.; Ha, S.; Joseph-McCarthy, D.; Kuchnir, L.; Kuczera, K.; Lau, F. T. K.; Mattos, C.; Michnick, S.; Ngo, T.; Nguyen, D. T.; Prodhom, B.; Reiher, W. E. III; Roux, B.; Schlenkrich, M.; Smith, J. C.; Stote, R.; Straub, J.; Watanabe, M.; Wiorkiewicz-Kuczera, J.; Yin, D.; Karplus, M. *J. Phys. Chem.* **1998**, *B102*, 3586.
(49) Suarez, D.; Brothers, E. N.; Merz, K. M., Jr. *Biochemistry* **2002**, *41*, 6615.
(50) Dal, Peraro, M.; Vila, A. J.; Carloni, P. *Inorg. Chem.* **2003**, *42*, 4245.
(51) Jorgensen, W. L.; Chandrasekhar, J.; Madura, J. D.; Impey, R. W.; Klein, M. L. *J. Chem. Phys.* **1983**, *79*, 926.
(52) Brooks, C. L., III; Karplus, M. *J. Mol. Biol.* **1989**, *208*, 159.
(53) Ryckaert, J. P.; Ciccotti, G.; Berendsen, H. J. *J. Comput. Phys.* **1977**, *23*, 327.
(54) Steinbach, P. J.; Brooks, B. R. *J. Comp. Chem.* **1994**, *15*, 667.
(55) Becke, A. D. *J. Chem. Phys.* **1993**, *98*, 5648.
(56) Lee, C.; Yang, W.; Parr, R. G. *Phys. Rev. B* **1988**, *37*, 785.
(57) Frisch, M. J.; Trucks, G. W.; Schlegel, H. B.; Scuseria, G. E.; Robb, M. A.; Cheeseman, J. R.; Montgomery, J. A.; T. V., Jr.; Kudin, K. N.; Burant, J. C.; Millam, J. M.; Iyengar, S. S.; Tomasi, J.; Barone, V.; Mennucci, B.; Cossi, M.; Scalmani, G.; Rega, N.; Petersson, G. A.; Nakatsuji, H.; Hada, M.; Ehara, M.; Toyota, K.; Fukuda, R.; Hasegawa, J.; Ishida, M.; Nakajima, T.; Honda, Y.; Kitao, O.; Nakai, H.; Klene, M.; Li, X.; Knox, J. E.; Hratchian, H. P.; Cross, J. B.; Adamo, C.; Jaramillo, J.; Gomperts, R.; Stratmann, R. E.; Yazyev, O.; Austin, A. J.; Cammi, R.; Pomelli, C.; Ochterski, J. W.; Ayala, P. Y.; Morokuma, K.; Voth, G. A.; Salvador, P.; Dannenberg, J. J.; Zakrzewski, V. G.; Dapprich, S.; Daniels, A. D.; Strain, M. C.; Farkas, O.; Malick, D. K.; Rabuck, A. D.; Raghavachari, K.; Foresman, J. B.; Ortiz, J. V.; Cui, Q.; Baboul, A. G.; Clifford, S.; Cioslowski, J.; Stefanov, B. B.; Liu, G.; Liashenko, A.; Piskorz, P.; Komaromi, I.; Martin, R. L.; Fox, D. J.; Keith, T.; Al-Laham, M. A.; Peng, C. Y.; Nanayakkara, A.; Challacombe, M.; Gill, P. M. W.; Johnson, B.; Chen, W.; Wong, M. W.; Gonzalez, C.; Pople, J. A. *Gaussian 03*, Revision A.1; Gaussian, Inc.: Pittsburgh, PA, 2003.
(58) Schaefer, P.; Riccardi, D.; Cui, Q. *J. Chem. Phys.* **2005**, *123*, 014905.
(59) Bicknell, R.; Schaffer, A.; Waley, S. G.; Auld, D. S. *Biochemistry* **1986**, *25*, 7208.
(60) Garrity, J. D.; Bennett, B.; Crowder, M. W. *Biochemistry* **2005**, *44*, 1078.
(61) Costello, A.; Periyannan, G.; Yang, K.-W.; Crowder, M. W.; Tierney, D. L. *J. Biol. Inorg. Chem.* **2006**, *11*, 351.
(62) Rasia, R. M.; Vila, A. J. *J. Biol. Chem.* **2004**, *279*, 26046.
(63) Concha, N. O.; Rasmussen, B. A.; Bush, K.; Herzberg, O. *Structure* **1996**, *4*, 823.
(64) Toney, J. H.; Fitzgerald, P. M.; Grover-Sharma, N.; Olsen, S. H.; May, W. J.; Sundelof, J. G.; Vanderwall, D., E.; Clearry, K. A.; Grant, S. K.; Wu, J. K.; Kozarich, J. W.; Pompliano, D. L.; Hammond, G. G. *Chem. Biol.* **1998**, *5*, 185.
(65) Kurosaki, H.; Yamaguchi, Y.; Higashi, T.; Soga, K.; Matsueda, S.; Yumoto, H.; Misumi, S.; Yamagata, Y.; Arakawa, Y.; Goto, M. *Angew. Chem., Int. Ed.* **2005**, *44*, 3861.
(66) Carenbauer, A. L.; Garrity, J. D.; Periyannan, G.; Yates, R. B.; Crowder, M. W. *BMC Biochem.* **2002**, *3*, 4.
(67) Garrity, J. D.; Pauff, J. M.; Crowder, M. W. *J. Biol. Chem.* **2004**, *279*, 39663.
(68) Simm, A. M.; Higgins, C. S.; Carenbauer, A. L.; Crowder, M. W.; Bateson, J.; Bennett, P. M.; Clarke, A. R.; Halford, S. E.; Walsh, T. R. *J. Biol. Chem.* **2002**, *277*, 24744.
(69) Suarez, D.; Diaz, N.; Merz, K. M., Jr. *J. Comput. Chem.* **2002**, *23*, 1587.
(70) Olsen, L.; Rasmussen, T.; Hemmingsen, L.; Ryde, U. *J. Phys. Chem. B* **2004**, *108*, 17639.
(71) Toney, J. H.; Hammond, G. G.; Fitzgerald, P. M.; Sharma, N.; Balkovec, J. M.; Rouen, G. P.; Olson, S. H.; Hammond, M. L.; Greenlee, M. L.; Gao, Y.-D. *J. Biol. Chem.* **2001**, *276*, 31913.
(72) Payne, D. J.; Hueso-Rodriguez, J. A.; Boyd, H.; Concha, N. O.; Janson, C. A.; Gilpin, M.; Bateson, J. H.; Cheever, C. A.; Niconovich, N. L.; Pearson, S.; Rittenhouse, S.; Tew, D.; Diez, E.; Perez, P.; De, la Fuente, J.; Rees, M.; Rivera-Sagredo, A. *Antimicrob. Agents Chemother.* **2002**, *46*, 1880.
(73) Garrity, J. D.; Carenbauer, A. L.; Herron, L. R.; Crowder, M. W. *J. Biol. Chem.* **2004**, *279*, 920.